Journal of Pharmaceutical Analysis 9 (2019) 133–141

Contents lists available at ScienceDirect

Journal of Pharmaceutical Analysis

journal homepage: www.elsevier.com/locate/jpa
www.sciencedirect.com

Original Article

Pharmacokinetic evaluation, molecular docking and in vitro biological evaluation of 1, 3, 4-oxadiazole derivatives as potent antioxidants and STAT3 inhibitors

Rashmin khanam [a], Iram I. Hejazi [a], Syed Shahabuddin [b], Abdul R. Bhat [c], Fareeda Athar [a,*]

[a] Centre for Interdisciplinary Research in Basic Sciences, Jamia Millia Islamia, New Delhi 110025, India
[b] Research Centre for Nano-Materials and Energy Technology (RCNMET), School of Science and Technology, Sunway University, 47500 Selangor, Malaysia
[c] Department of Chemistry, Sri Pratap College, Cluster University, Srinagar 190001, India

ARTICLE INFO

Article history:
Received 13 March 2018
Received in revised form
1 December 2018
Accepted 4 December 2018
Available online 7 December 2018

Keywords:
1, 3, 4-oxadiazoles
Structure-activity relationship (SAR)
Antioxidant activities
STAT3 inhibitors
Molecular docking

ABSTRACT

1, 3, 4-Oxadiazole derivatives **(4a–5f)** were previously synthesized to investigate their anticancer properties. However, studies relating to their antioxidant potential and signal transducer and activator of transcription (STAT) inhibition have not been performed. We investigated previously synthesized 1, 3, 4-oxadiazole derivatives (**4a–5f)** for various radical scavenging properties using several in vitro antioxidant assays and also for direct inhibition of STAT3 through molecular docking. The data obtained from various antioxidant assays such as 2, 2,-diphenyl-1-picrylhydrazyl radical (DPPH), nitric oxide, hydrogen peroxide, and superoxide anion radical revealed that among all the derivatives, compound **5e** displayed high antioxidant activities than the standard antioxidant L-ascorbic acid. Additionally, the total reduction assay and antioxidant capacity assay further confirmed the antioxidant potential of compound **5e**. Furthermore, the molecular docking studies performed for all derivatives along with the standard inhibitor STX-0119 showed that binding energy released in direct binding with the SH2 domain of STAT3 was the highest for compound **5e** (-9.91kcal/mol). Through virtual screening, compound **5e** was found to exhibit optimum competency in inhibiting STAT3 activity. Compound **5e** decreased the activation of STAT3 as observed with Western blot. In brief, compound **5e** was identified as a potent antioxidant agent and STAT3 inhibitor and effective agent for cancer treatment.

1. Introduction

In a previous investigation on 5-aryl-2-butylthio-1, 3, 4-oxadiazole derivatives (**4a–5f**), we observed antiproliferative effects of these compounds on MCF-7 breast cancer cells as a result of the induction of apoptosis [1]. In the present study, we further explored the potential of these compounds as antioxidants and STAT3 inhibitors through computational analyses to establish the authenticity of these derivatives as potent anticancer agents because antioxidants and STAT3 inhibitors are known to play prominent roles against the progression of cancer.

Reactive oxygen species (ROS) such as superoxide, singlet oxygen, hydroxyl radical and hydrogen peroxide produced under oxidative stress damage various biological macromolecules, causing serious health problems such as cancer, inflammation, cardiovascular and neurodegenerative disorders [2,3]. Thus, effective antioxidants are needed as they inhibit the survival and proliferation of cancer cells by reducing the oxidative stress [4].

Because of the possibility of simple transfer of hydrogen atom and resonance stability of the resulting carboxylate radical, the substituted benzoic acid could inhibit the formation of free radical species by reducing oxidation [5]. The derivatives of benzoic acid are found in various natural and synthetic antioxidants such as chalcones, flavones, salicylic acid and parabens [6]. 2, 5-disubstituted-1, 3, 4-oxadiazole exhibits a wide spectrum of biological activities [7]. As reported earlier, many derivatives containing the 1, 3, 4-oxadiazole moiety including sulfonamidomethane [8], benzoxazole [9], pyrimidines [10] and methoxyphenyl [11] display significant antioxidant properties. Thus taking into consideration the antioxidant properties of benzoic acid and 1, 3, 4-oxadiazoles scaffold, new derivatives (**4a–5f**) containing the 1, 3, 4-oxadiazole ring formed through cyclization of derivatives of benzoic acid synthesized in our previous study could serve as potent anticancer agents by effectively scavenging the free radical formation because of extended conjugation and stability.

Signal transducer and activator of transcription (STAT) comprises a group of seven proteins, namely, STAT1, 2, 3, 4, 5a, 5b and 6. STAT3 is closely related to the occurrence of cancers [12]. Many

Peer review under responsibility of Xi'an Jiaotong University.
* Corresponding author.
E-mail address: fathar@jmi.ac.in (F. Athar).

https://doi.org/10.1016/j.jpha.2018.12.002

cancers, such as those of breast, prostate, lung and ovaries, as well as leukemia and lymphoma, occur due to the abnormal activation of STAT3 [13,14]. STAT3 acts as a prime factor in the regulation of many cellular events involving cell proliferation, differentiation, apoptosis and angiogenesis [13,15–17] and, therefore, an inhibitor of STAT3 activation could be an interesting lead for cancer drug discovery [18–21].

The 1, 3, 4-oxadiazole scaffold is extensively used in the inhibition of STAT3 in various cancer cells. Dell'Orto et al. [22] showed that an oxadiazole based compound effectively inhibited the activation of STAT3 by targeting the STAT3-SH2 domain in a dose-dependent manner. Shin et al. [23] reported that oxadiazoles containing ureido derivatives inhibited STAT3 signaling by blocking the upstream tyrosine kinases involved in the activation of STAT3. Matsuno et al. [24] reported the inhibition of dimerization of STAT3 through STX-0119 (an oxadiazole derivative) in several cancer cell lines. Using the virtual screening approach, the ability of the synthesized compounds **(4a–5f)** as effective STAT3 inhibitors through direct binding to the STAT3-SH2 domain, and thereby blocking the dimerization and activation of STAT3, was investigated.

2. Materials and methods

2.1. Chemicals and software

All the chemicals were of the highest quality available. The reagents used in experiments including L-Ascorbic acid, 2, 2-diphenyl-1-picrylhydrazyl (DPPH), Griess reagent, sodium nitroprusside, Tris-HCl buffer, dimethyl sulfoxide (DMSO), and hydrogen peroxide, were purchased from Sigma Aldrich (India). The human cell line MCF-7 (breast cancer cell line) was procured from National Centre for Cell Science (Pune, India). The cells were cultured in Roswell Park Memorial Institute (RPMI)-1640 medium containing 10% fetal bovine serum along with 1% penicillin–streptomycin–neomycin (GIBCO Grand Island, New York, USA) in a humidified atmosphere having 5% CO_2 maintained at 37 °C. All the computational studies were performed using Windows 10 Professional on a personal computer with Intel Core i3microprocessor, 4 GB RAM and a 64-Bit operating system. We used biological databanks such as PubChem, and Protein Data Bank (PDB) and online tools such as Online Pass Server along with softwares like Chemdraw Ultra 8.0, AutoDock 4.2, and Discovery Studio version 3.5.

2.2. In vitro antioxidant assays

2.2.1. DPPH radical scavenging assay

The antioxidant property of the synthesized compounds was evaluated through free radical scavenging assay by observing the changes in optical density of DPPH radicals. One milliliter of synthesized compounds in the concentration range of 0–100 μg/mL dissolved in methanol were added to 5 mL of 0.005% (w/v) methanol solution containing DPPH. After incubating for 30 min at room temperature, the absorbance was measured at 519 nm. Ascorbic acid was taken as a standard. All the experiments were repeated thrice.

2.2.2. Nitric oxide radical scavenging activity

The nitric oxide (NO) radical scavenging ability was evaluated using slight changes in the methods employed by Green et al. [25] and Marcocci et al. [26]. The tested compounds were taken in a concentration range of 0–100 μg/mL, and added to the solution containing 1.2 mL of sodium nitroprusside (10 mM) and 1.7 mL of phosphate buffer saline (0.2 M, pH 7.6); the mixture was left for incubation for 152 min at 25 °C. Following incubation, 1 mL of Griess reagent was used to treat 1 mL of reaction mixture and the absorbance was measured at 545 nm. Ascorbic acid was taken as a standard antioxidant. The NO scavenging activity was calculated using the following equation:

$$\%\ \text{of NO scavenging} = \left[\frac{A_{control} - A_{sample}}{A_{blank}}\right] \times 100$$

where $A_{control}$, A_{sample} and A_{blank} represent the absorbance of the control reaction (reagents and ascorbic acid), test compound (reagents and synthesized compounds) and blank (reagents only). All experiments were carried out in triplicates.

2.2.3. H_2O_2 scavenging activity

Forty millimolar of H_2O_2 solution was prepared in phosphate buffer (50 mM, pH 7.4) [27]. All the synthesized compounds in the concentration range of 0–100 μg/mL containing 3.5 mL phosphate buffer were added to 0.5 mL of H_2O_2 solution. The absorbance of the reaction mixture was measured at 232 nm. Ascorbic acid was used a reference. All experiments were repeated thrice.

2.2.4. O_2^- scavenging activity

In brief, 1.2 mL of test compounds were added to 7 mL of 5 mM Tris-HCl buffer (pH 8.3) [28]. Forty-two microliters of 4.4 mM of pyrogallol was added to the reaction mixture. The mixture was stirred and a single drop of ascorbic acid was added after 5 min. The absorbance was measured at 450 nm. All the experiments were repeated thrice.

2.2.5. Total reduction capacity and total antioxidant activity

The method of Oyaizu et al. [29] was used to determine the total reduction capacity with some modifications. In brief, 2.52 mL of 0.2 M phosphate buffer (pH 6.8) along with 1% (w/v) $K_3Fe(CN)_6$ was added to 1.5 mL of test compounds dissolved in distilled water. After incubating the reaction mixture for 20 min at 50 °C, 2.6 mL of 10% (w/v) trichloro acetic acid was added. The mixture was then centrifuged at 3000 rpm for 15 min to separate and collect the top layer of the solution, which was then mixed with distilled water and 0.76 mL of 0.1% (w/v) $FeCl_3$. All the absorbance values were taken at 695 nm. The method of Prieto et al. [30] with some modifications was employed to calculate the total antioxidant activity. In brief, 0.2 mL of test sample (200 μg) was mixed with 1.5 mL of the reagent (0.5 M H_2SO_4, 25 mM Na_2PO_3 and 4.5 mM ammonium molybdate). The tube was capped and incubated in a boiling water bath at 95 °C for 90 min. The samples were cooled to room temperature and absorbance of the solution was read with reference to the blank at 690 nm using UV spectrophotometer.

2.3. In silico pharmacokinetics analysis for STAT3 inhibition

2.3.1. Molecular modeling analysis

The molecular docking study was performed using the software AutoDockTools (ADT) version 1.5.6 taken from the Scripps Research Institute [31]. The X-ray 3D crystal structure of STAT3 with a ligand (PDB ID: 1BG1) was retrieved from the RSCB Protein Data Bank (web address: http://www.rscb.org/pdb/) and was used as a docking receptor.

2.3.2. Preparation of ligands and receptors

To propose new inhibitors, the build-and-edit module of Chemdraw ultra 12.0 was used. It was used to draw the structures of ligands, which were then converted into PDB file. The PDB ligand files, thus obtained were converted to PDBQT file using ADT version 1.56, which helped in the conversion by detecting the root, choosing the torsion and setting the torsion numbers. The structure was made free from all the co-crystallized ligands and water

molecules. Using ADT, all the polar hydrogen atoms were added. This was followed by the removal of residue structures and replacement of all incomplete side chains [31]. The Gasteiger charges were added to each atom and non-polar hydrogen atoms were dissolved with the structure of protein. All the structures were saved in PDBQT files for further evaluation using ADT.

2.3.3. Molecular docking

The Lamarckian genetic algorithm was employed with the help of AutoDock 4.2 software to perform the docking study of the ligand molecules with STAT3 (PDB ID: 1BG1) [32]. Auto grid was used to calculate the center of the active site pocket for the ligand which is represented by the grid maps [33]. The dimensions of the grid for STAT3 protein were 80 × 80 × 80 grid points with spacing of 0.750 Å between the grid points but centered on the ligand for receptor (101.36, 87.332 and 31.445 coordinates). Based on the values of binding energy (kcal/mol) and inhibition constant (ki) value (μM), the best docked conformation was selected. The final results, thus obtained featuring hydrogen and hydrophobic interactions of the docked compounds with the modeled structures, were interpreted using PyMOL software.

2.3.4. Evaluation of the ADMET and TOPKAT properties

The absorption, distribution, metabolism, excretion and toxicity (ADMET) properties for the synthesized compounds were evaluated using Discovery Studio 3.5 (Accelrys San Diego, USA) as evaluation of these properties before designing a drug plays a crucial role in clinical phases [34]. The after effects of drug intake were assessed using TOPKAT, which helps in determining the toxicological final points using quantitative structure-toxicity relationship (QSTR).

2.3.5. Biological activity spectrum (BAS)

To evaluate the pharmacological properties of the best docked compounds (4e, 4f, 5e and 5f), the biological activity spectrum (BAS) was determined. It is useful software for determining the pharmacological properties as these properties are related to the structural properties. The pharmacological properties of a compound and its association with the biological system were assessed using PASS by uploading the SMILES string of the respective compounds online.

2.3.6. Alpha screen based assay

It is a bead-based nonradioactive assay carried out in a microtiter plate and is used to elucidate the biomolecular interactions [35]. Forty millimeters of the reaction mixture was taken in a 96-well plate containing 13 mM HEPES-NaOH (pH 7.2), 65 mM NaCl , 1 mM EDTA (pH 7.6), 0.1% NP- 40 and 10 mg/mL BSA at 25 °C. The Phospho-Tyr (p-Tyr) peptide fragment used in this study was 5-carboxyfluorescein (FITC)-GpYLPQTV for STAT3. The SH2 and 80 μM protein were incubated with the compound for 20 min. The protein and the FITC-pTyr peptide were incubated for 90 min. The streptavidin coated donor beads and anti-FITC acceptor beads were mixed and reading was taken at 575 nm using EnVison Xcite (Perkin Elmer).

2.4. Western blot analysis

The Western blot analysis was carried out using a previously described protocol after some modifications [36]. The MCF-7 cells were cultured in RPMI-1640 medium supplemented with 10% FBS purchased from GIBCO Grand Island, New York, USA. The cells were seeded in six-well plates and cultured overnight to allow them to become confluent. The medium in the plate was changed with fresh medium containing 10% FBS (control) and compound **5e** at different concentrations after 24 h. The cell lysate was prepared using the lysis buffer containing the protease and phosphatase inhibitors. Total protein was extracted and protein estimation was done using Bradford reagent. The total protein (70 μg) was loaded on a 12% SDS polyacrylamide gel and blotted onto a PVDF membrane after electrophoresis. The blocking of membrane was done, using the 5% BSA, and then the membrane was incubated overnight in STAT3 (Cat no. SC-482) primary antibody at a dilution of 1:1000 at 4 °C. The blot was subsequently washed thrice using TBS-T and incubated for 1 h at room temperature with the secondary antibody (Cat no. SC-2030). Images were visualized with the LAS-4000 using the ECL reagent. All the important reagents were purchased from Sigma Aldrich (India) while primary STAT3 and secondary antibodies were brought from Santa Cruz Biotechnology, Texas, USA.

2.5. Statistical analysis

All the experimental data are presented as means ± SD of triplicate results. The data were analyzed using unpaired Student's *t*-test to calculate the *P* values (value of significance) with the GraphPad Prism version 7.0 software (San Diego, CA, USA). The *P* values < 0.05 were considered statistically significant.

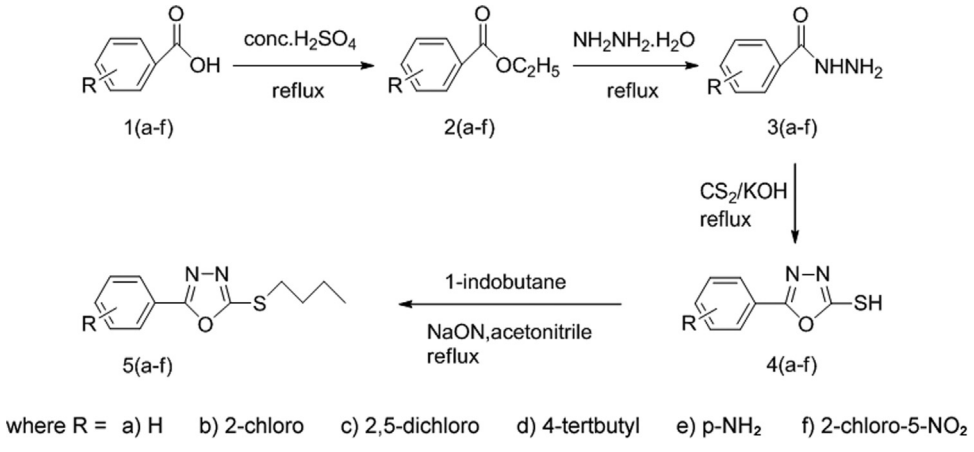

Scheme 1. Schematic representation for synthesis protocol for compounds (**4a–5f**).

Table 1
The IC50 values (μM) of synthesized compounds (**4a–5f**) calculated from various in vitro antioxidant assays[a].

Compound No.	R	DPPH	NO	O_2^-	H_2O_2
4a	H, H	89.96 ± 3.4	112.10 ± 2.3	165.01 ± 3.2	121.03 ± 4.4
4b	Cl; H	74.07 ± 3.3	79.31 ± 3.1	142.04 ± 1.1	105.48 ± 3.4
4c	Cl, Cl; H	83.57 ± 1.1	101.03 ± 4.1	141.92 ± 1.2	107.06 ± 1.1
4d	tertbutyl; H	56.90 ± 3.3	94.39 ± 2.2	83.23 ± 3.2	117.01 ± 3.3
4e	NH_2; H	**47.04 ± 2.2**	**44.05 ± 3.0**	**50.81 ± 2.2**	**47.72 ± 3.3**
4f	Cl, NO_2; H	**54.07 ± 3.9**	**47.72 ± 1.1**	**48.07 ± 1.9**	**46.58 ± 1.5**
5a	H; n-butyl	62.11 ± 3.8	110.30 ± 5.1	164.47 ± 3.4	90.09 ± 2.2
5b	Cl; n-butyl	68.18 ± 5.1	63.85 ± 4.4	134.77 ± 4.4	61.85 ± 1.3
5c	Cl, Cl; n-butyl	64.18 ± 4.4	89.92 ± 1.3	84.88 ± 2.2	50.34 ± 3.2
5d	tert-butyl;n-butyl	71.63 ± 2.8	76.45 ± 1.1	107.75 ± 3.3	50.01 ± 3.1
5e	**NH_2; n-butyl**	**30.65 ± 4.2**	**38.49 ± 6.1**	**40.98 ± 1.9**	**40.65 ± 2.2**
5f	**Cl, NO_2; n-butyl**	**44.62 ± 5.5**	**39.16 ± 2.2**	**45.52 ± 1.2**	**44.64 ± 1.1**
L-Ascorbic acid[b]	–	31.26 ± 2.3	38.93 ± 2.5	39.96 ± 1.2	41.04 ± 3.1

[a] IC50: concentration of compound required to inhibit radical formation by 50%. Values (in μM) are expressed as mean ± SD for a set of three experiments.
[b] L-Ascorbic acid: standard antioxidant drug used for comparison.
Bold values represent the active compounds.

3. Results and discussion

3.1. In vitro antioxidant activity

The synthesized compounds (Scheme 1) (**4a–5f**) reported by us previously [1] were tested for their antioxidant potential using the DPPH [37], NO [38], H_2O_2 [2], O_2^- [39], total reducing capacity [2] and total antioxidant assays [40]. The results for the in-vitro antioxidant assays for the synthesized compounds and the standard antioxidant were compared.

3.1.1. DPPH radical scavenging activity

The DPPH radical scavenging activity of all the synthesized compounds (**4a–5f**) was evaluated and is presented in Table 1. It was observed that among all the compounds **4e**, **4f**, **5e** and **5f** had effective antioxidant activities. In particular, the compound **5e** showed an IC_{50} values that was very close to the IC_{50} value of the standard antioxidant, L-ascorbic acid. The higher scavenging ability of the compound **5e** relative to those of other compounds was a result of the high resonance stability of radical being formed after heterolytic cleavage delocalizing through the aromatic and 1, 3, 4-oxadiazole rings (Scheme 2). The compounds substituted with butyl hydrocarbon chain (**5a–f**) exhibited higher antioxidant activities than the compounds with a free mercapto group (**4a–f**), suggesting that the presence of an alkyl chain at C-2 further enhanced their activities [41]. The compound **5e** showed 89.90% inhibition of the DPPH radical at a concentration of 80 μg/mL. The inhibition percentage of the DPPH radical was found to be 35.24%, 48.54% and 77.38% at ½ × IC_{50}, IC_{50} and 2 × IC_{50} concentrations of the compound **5e**, respectively. Moreover, the radical scavenging activity of the compound **5e** and L-ascorbic acid was not statistically significant ($P > 0.05$) in the concentration range of 50–80 μg/mL (Fig. 1A).

3.1.2. NO radical scavenging activity

The NO scavenging activities for all the tested compounds and the reference drug are shown in Table 1. From the data, it is clear that the compounds showing considerable DPPH scavenging activity also exhibited significant NO scavenging activity. Owing to the resonance stability and the inductive effect of the -NH_2 group at para position to the benzene ring, compound **5e** exhibited the most significant antioxidant activity, which was not statistically significant compared with that of the standard antioxidant ($P > 0.05$) (Fig. 1B).

3.1.3. H_2O_2 scavenging activity

H_2O_2 is an oxidizing species present in many animal tissues. It is a biologically important reagent because it diffuses across many biological membranes, bringing oxidative damage to DNA, lipids and protein molecules. As represented in Table 1, among all the compounds, four compounds, namely, **4e**, **4f**, **5e,** and **5f**, exhibited significant H_2O_2 scavenging that was almost similar to that obtained for L-ascorbic acid at its IC_{50} in contrast to the low H_2O_2 activities previously reported for compounds having 1, 3, 4-oxadiazole ring [2]. In particular, the compound **5e** exhibited a prominent antioxidant activity because of low bond dissociation energy for the -NH_2 group [42] and showed increased scavenging of (OOH.) radicals in a concentration-dependent manner without significant statistical difference ($P > 0.05$). The H_2O_2 scavenging activity for the compound **5e** at ½ × IC_{50}, IC_{50} and 2 × IC_{50} concentrations was found to be 42.6%, 58.04% and 81.90%, respectively (Fig. 1C).

3.1.4. O_2^- scavenging activity

O_2^- radical is very reactive and acts as a biological catalyst in the reduction of molecular oxygen [39]. As shown in Table 1, the

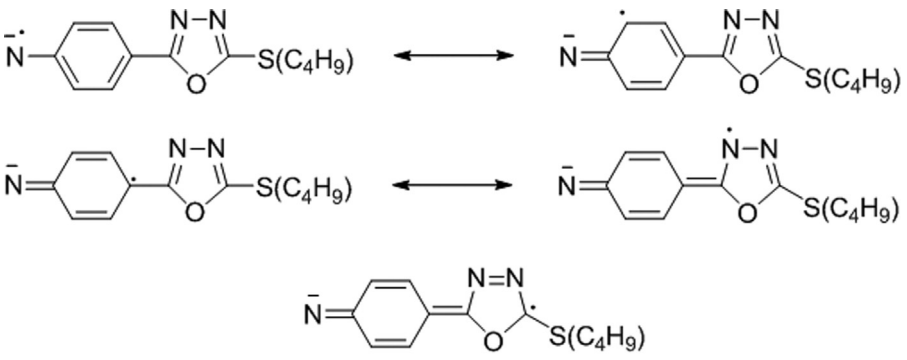

Scheme 2. Resonance stabilization of radical formed from compound **5e** after heterolytic cleavage.

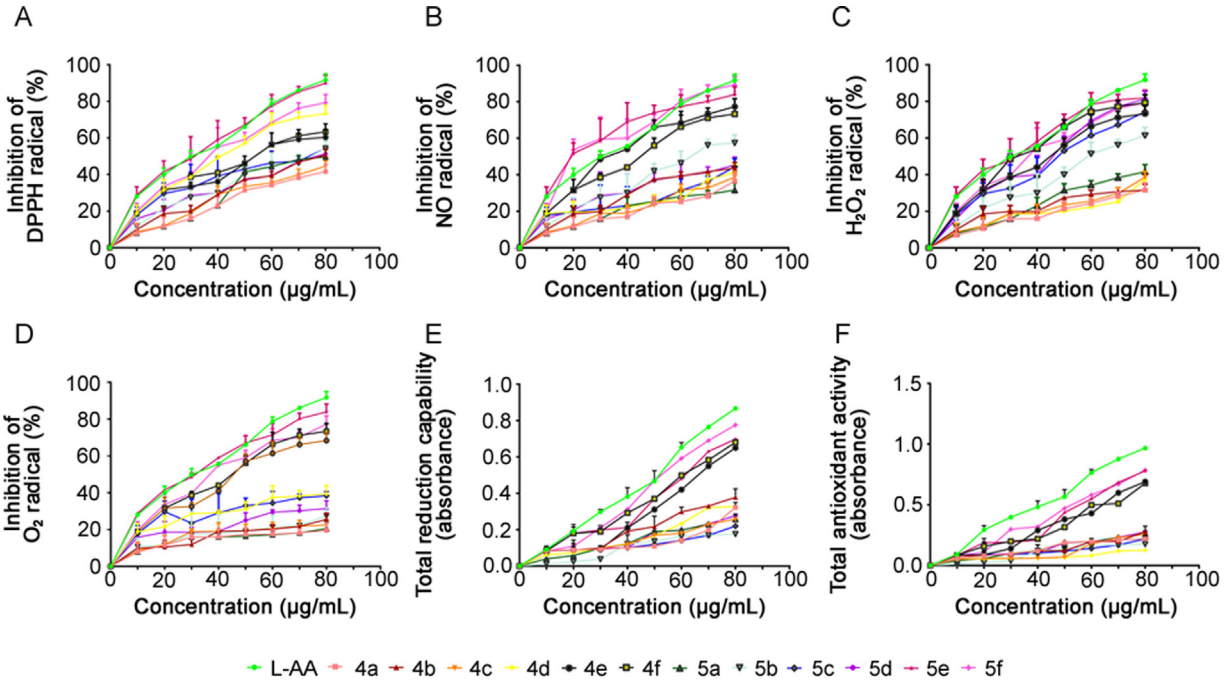

Fig. 1. Percentage inhibition of radicals of compounds **(4a–5f)** using different in-vitro antioxidant assays. (A) DPPH, (B) nitric oxide radical, (C) hydrogen peroxide radical, (D) superoxide anion radical, (E) total reduction capacity assay, and (F) total antioxidant capacity assay. L-ascorbic acid is taken as the standard antioxidant. Values are expressed as mean ± SD for a set of three experiments.

IC_{50} value for the compound **5e** was almost equal to that of L-ascorbic acid. As revealed from Fig. 1D, at higher concentrations the compound **5e** inhibited the formation of O_2^- radical up to 83.9%, thus displaying a significant potential as an antioxidant. Furthermore, it was observed that the percentage of inhibition of radicals by the compound **5e** and L-ascorbic acid was not statistically different ($P > 0.05$) within the concentration range of 10–80 μg/mL.

3.1.5. Total reduction capacity and total antioxidant capacity

The total reduction capacity and total antioxidant capacity of all the synthesized compounds (**4a–5f**) and L-ascorbic acid are presented in terms of the optical densities in the concentration range of 0–100 μg/mL in Fig. 1E and Fig. 1F, respectively. Both the assays revealed that only four compounds, namely, **4e**, **4f**, **5e** and **5f**, showed better results for the total reduction capacity and total antioxidant capacity ($P > 0.05$) in terms of absorbance in a concentration-dependent manner. Particularly, the compound **5e** exhibited the highest activity throughout.

3.1.6. Structure-activity relationship (SAR)

The data obtained from in vitro antioxidant assays for the synthesized compounds (**4a–5f**) showed that the presence of various substituents on the phenyl ring at C-5 and the alkyl group at C-2 of the 1, 3, 4-oxadiazole ring is important in determining the SAR. The possible reason for the increased antioxidant activity for compounds **5a–5f** compared to that for **4a–4f** was the presence of the hydrocarbon chain. The prominent radical scavenging activity of the compounds **4e** and **5e** was due to the high inductive (+I effect) and mesomeric effects (+M effect) of a strong electron donating (-NH_2) group at para position to the phenyl ring. The plausible reason for the antioxidant activity of compounds **4f** and **5f** might be the presence of strong electron withdrawing group (-NO_2) at the meta position. No significant activity was exhibited by the compounds **4a**–**4d** and **5a**–**5d**, which could presumably be due to the presence of weak electron donating (alkyl) and withdrawing (-chloro) groups.

3.2. In silico pharmacokinetic analysis for STAT3 inhibition

3.2.1. Molecular docking

The synthesized compounds (**4a–5f**) and the known inhibitor STX-0119 were analyzed by molecular docking using the rigid docking method [31]. AutoDock 4.2 was used to determine the orientation of inhibitors bound in the active site of STAT3 (PDB ID: 1BG1) and also to determine the conformation exhibiting the highest binding energy value for each molecule. With the aim of developing new STAT3 inhibitors, the binding modes for STAT3 inhibitors were analyzed using the PyMOL software. The binding site in the SH2 domain of STAT3 as described by Becker et al. [43] was used to elucidate the interactions, contributing to the binding affinity of new inhibitors, which can be used to design potent inhibitors.

The active residue sites for SH2 domain of STAT3 were Leu 438, Asp 369, Arg 382, Gly 442, Arg 423, His 457, Lys 244, Glu 444, Thr 443, Thr 456 and Lys 244 as analyzed by DoGsiteScorer server. We designed the STAT3 inhibitors having 1, 3, 4-oxadiazole ring with different phenyl substituents having free mercapto group (**4a–f**) and butyl chain attached to a sulfur atom forming butyl-mercapto linker (5a–f) (Scheme 1). These compounds sufficiently act as H-bond acceptors as well as donors due to the presence of various polar linkages such as C-O-C, N=C-O and C=S, acting as hydrophobic and hydrophilic sites in the form of these dipoles.

Docking results showed that all compounds (**4a–f**) with a free -SH group exhibited similar orientations in the binding pocket of the SH2 domain of STAT3. However, compounds substituted with the butyl mercapto linkage exhibited different conformational behaviors because of their diverse atomic compositions and chemical properties. To explore the SAR profile, the role of alkyl linkage (**5a–f**) and free –SH group (**4a–f**) at C-2 of 1, 3, 4-oxadiazole ring with substituted phenyl ring at C-5 was analyzed. The compound **4a** bearing an unsubstituted phenyl ring at C-5 formed three H-bonds: the first H-bond formed between the –C-O-C-linkage of oxadiazole ring and Ser 372 residue with a bond distance of 3.5 Å, while the other two H-bonds formed between

Table 2
Binding energy and specific interaction of STAT3 with the synthesized compounds.

Compound no.	Binding energy (kcal/mol)	Inhibitory constant (μM)	Protein ligands interaction		
			No. of H bonds	Amino acid residues	Distance (Å)
4a	− 4.58	442.52	3	Ser372 Leu438 Thr440	3.5 1.1 1.9
4b	− 5.48	110.16	2	His457 Lys244	2.9 3.4
4c	− 5.18	249.97	–	–	–
4d	− 5.25	239.70	–	–	–
4e	− 8.04	16.50	6	His457 Thr456 Lys244	2.9, 3.1 2.6, 3.1 2.6, 1.7
4f	− 7.82	19.19	3	Asp566 Asp334	3.5 3.3, 3.1
5a	− 5.68	98.59	2	Arg379	3.2, 3.4
5b	− 5.89	91.79	2	Arg335	3.1, 3.3
5c	− 5.20	210.36	0	–	–
5d	− 5.30	241.44	0	–	–
5e	− 9.91	10.36	6	Thr456 His457 Lys244 Gln247	3.0, 2.6 3.4, 3.0 3.4 2.0
5f	− 8.81	14.21	3	Gly380 Gly442 Arg423	2.9 3.0 3.0
STX-0119	− 6.37	21.30	3	Glu415 Gln416	2.0 3.5, 3.2

the -N=C-O- linkage of oxadiazole moiety and Thr 440, and Leu 438 residues with a bond distance of 1.1 Å and 1.9 Å, respectively. For compound **5a,** the –N=C-O- linkage of oxadiazole ring formed two H-bonds with Arg 379 residues with a bond distance of (3.2 Å, 3.4 Å) and one pi-interaction. The compound **4b**, having o-Cl atom, also formed 2 H-bonds but no pi-interaction with His 457 or Lys 244 was observed. Compound **5b** showed 2 H-bonds and one pi-interaction with Arg 335 with bond distance of 3.1 Å and 3.3 Å, respectively. The 2, 4-dichloro and para- tert-butyl group of compounds **4c** and **4d**, respectively formed no hydrogen bond and no pi-interaction with amino acid residues. Compounds **5c** and **5d** also interacted in a similar way as compounds **4c** and **4d** respectively did not show any interaction. The compound **4e** having a p-amino group formed 6 H-bonds with His 457 (2.3 Å, 3.3 Å), Thr 456 (2.9 Å, 3.1 Å) and Lys 244 (2.6 Å, 1.7 Å) residues and two pi-interaction with Thr 456 and His 457 residues respectively. Compound **5e** with a p-amino group and butyl mercapto linkage at C-2 showed 6 H-bond interaction with Thr 456 (3.0 Å, 2.6 Å), His 457 (3.4 Å, 3.0 Å), Lys 244 (3.4 Å) and Gln 247 (2.0 Å) residues and one pi-interaction with Thr 456 residue. Compound **4f** with nitro and chloro group formed 3 H-bonds with two amino acid residues, Asp 566 (3.5 Å) and Asp 334 (3.3 Å, 3.1 Å), while compound **5f**formed 3 H-bonds with Gly 380 (2.9Å), Gly 442 (3.0 Å) and Arg 423 (3.0 Å) residues (Table 2).

Thus, on the basis of SAR studies it can be inferred that an amino group at para position of the phenyl ring of compound **4e** and a butyl mercapto linkage at C-2 present in compound **5e** in comparison to other compounds were more interactive and competent in forming stable protein-ligand complex. In general, compound **5e** interacted with residues Thr 456 (3.0 Å, 2.6 Å), His 457 (3.4 Å, 3.0 Å), Lys 244 (3.4 Å) and Gln 247 (2.6 Å) through H-bonds and with Thr 456 residue through pi-interaction (Fig. 2 C and D) in comparison to the standard drug (STX-0119)Fig. 2 A and B), where the pi-interactions were absent and only H-bonds could be formed with Glu 415 (2.0 Å) and Gln 416 (3.5 Å and 3.2 Å) residues.

3.2.2. ADMET and TOPKAT prediction

The in-silico profile of the selected compounds (**4e**, **4f**, **5e** and **5d**) was evaluated to determine their putative bioavailability as STAT3 inhibitors. Physicochemical properties, primarily aqueous solubility (logS), lipophilicity (clogP), molecular weight (MW) and polar surface area, linearly correspond to the bioavailability and absorption of a drug molecule. CYPs (cytochrome P450) play an important role in drug metabolism and also determine the nature of drugs inside the body. AlogP value (lipophilicity) is a significant property for calculating oral bioavailability of a drug. Here, we employed ADMET (DS3.5) to evaluate the predicted pharmacokinetic profile of compounds by using the standard inhibitor STX-0119. The results showed that all the synthesized compounds **4e**, **4f**, **5e** and **5f** had standard AlogP value $\leq$ 5. Similarly, the compounds **4e**, **4f**, **5e** and **5f** showed moderate to good solubility (solubility level = 3). The observed value of human intestinal absorption (HIA) was excellent for entire molecules. The penetration ability of compounds across the blood-brain-barrier (BBB) was high when prediction value was zero and low when the value was 4. All four compounds showed better BBB penetration ability; however, only two compounds **5e** and **5f** exhibited probability score for hepatotoxicity $\leq$ 0.5. All four compounds had good HIA value. Except for compounds **5e** and **5f**, the other two compounds

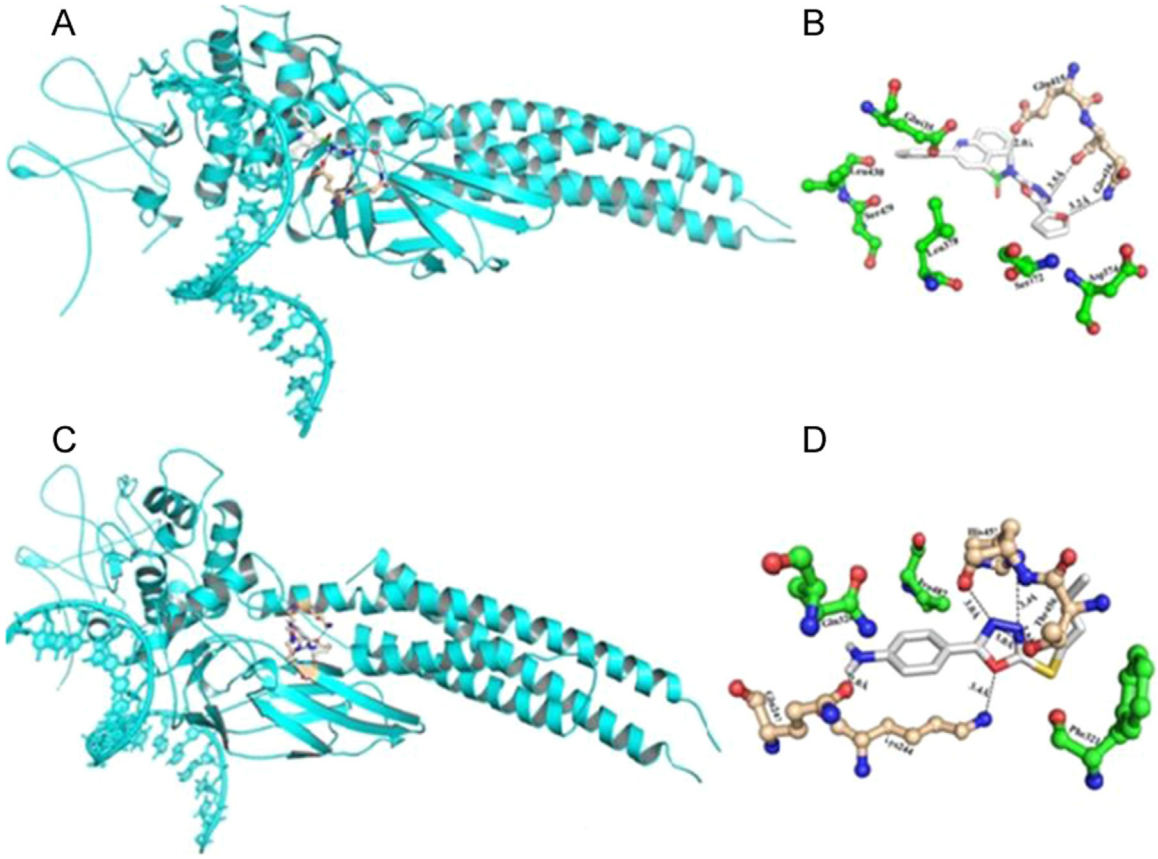

Fig. 2. Docked conformations of the known inhibitor STX-0119 (A and B) and compound 5e (C and D) into the active site of STAT3 binding pocket.

were active against CYP2D6 enzyme. For real drug ability, the ideal plasma protein binding (PPB) level is 0. Except for compound **5e**, all the compounds showed poor PPB. Polar surface area (PSA) depends on the conformation and hydrogen bonding. For a drug to be active, the optimum value of PSA is $\leq$ 140 Å. All predicted compounds showed significant PSA.

With the help of the computer-aided toxicity predictor, TOPKAT, the cellular toxicity of compounds **4e**, **4f**, **5e** and **5f** was determined after comparison with a known STAT3 inhibitor. The carcinogenic and mutagenic effects of compounds determined using weight of evidence (WOE Prediction) and Ames Prediction were prime factors. These techniques consist of various toxic endpoints and models (irritation, teratogenicity, sensitization, neurotoxicity and immunotoxicology) that are useful in drug development. All the selected compounds showed Ames probability score $\leq$ 7 and were found to be mutagenic except for compounds **5e** and **5f**. WOE, another toxicity predictor, is used to evaluate the relative level of a compound that causes cancer in humans. All compounds expect **5e** and **5f** were carcinogenic (Table 3).

ADMET and TOPKAT properties for the selected compounds **4e**, **4f**, **5e** and **5f** along with the known inhibitor suggested that among the four compounds, compound **5e** emerged as the lead for STAT3 inhibition.

3.2.3. *Biological activity spectrum (BAS)*

PASS online server was used to evaluate the related biological activities for selected compounds. As these probabilities can be independently evaluated, the Pa and Pi values ranged from 0 to 1 and Pa + Pi was $<$ 1. The Pa represents the active compounds while Pi represents inactive compounds [44]. The data from PASS prediction showed that the values for Pa were found to be higher than Pi values, suggesting inhibition of transcription factor involved in activation of STAT3 protein. All the four compounds **4e**, **4f**, **5e** and **5f** inhibited the transcription factor involved in the activation of STAT3 within the range of 0.607–0.746. Compound **5e**, in particular, exhibited significant Pa values in comparison to other compounds (Table 4).

Table 3
Pharmacokinetic profiles of known inhibitors and synthesized compounds[a].

Pharmacokinetic profiles	Synthesized compounds				STX-0119
	4e	4f	5e	5f	
ADMET					
BBB	3	3	2	2	2
AlogP	1.284	2.589	2.794	4.100	3.983
Sol.	3	3	3	2	2
HIA	0	0	0	0	0
HTL	1	1	1	0	1
HT_Prob	0.94	0.68	0.50	0.45	0.98
PPB	1	0	2	1	2
CYP2D6	0	0	1	1	1
PSA	61.61	77.89	61.61	77.89	89.00
TOPKAT					
Ames Mut.	M	M	NM	NM	M
Prob	0.76	0.77	0.70	0.71	0.78
Enrichment	1.37	1.38	1.26	1.27	1.39
WOE	C	C	NC	NC	C

[a] BBB: blood brain barrier level value: 0 (high penetration); 1 (no penetration), HIA: human intestinal absorption level value: 0 (good); 1(moderate), Sol. (solubility level): 3, HTL: hepatotoxicity level value: 0 (good); 1 (moderate), HT-Prob.: hepatotoxicity probability $<$ 0.5 is ideal, CYP2D6 $<$ 0.5 is good and denoted as level 0, PPB: plasma protein binding value $\leq$0, AlogP value $\leq$5.0 and Polar surface area $\leq$ 140. Ames Mut.: Ames mutagen prediction, Prob.: Ames probability; Enrichment: Ames enrichment; WOE-Prediction (weight of evidence); M: (mutagen); NM: (non-mutagen); C: (carcinogen); NC: (non-carcinogen).

Table 4
Biological activity spectrum of compounds (Pa – Active; Pi – Inactive).

Compounds	Pa	Pi	Activity
4e	0.676	0.004	Transcription factor STAT3 inhibitor
4f	0.607	0.006	Transcription factor STAT3 inhibitor
5e	0.746	0.004	Transcription factor STAT3 inhibitor
5f	0.609	0.006	Transcription factor STAT3 inhibitor

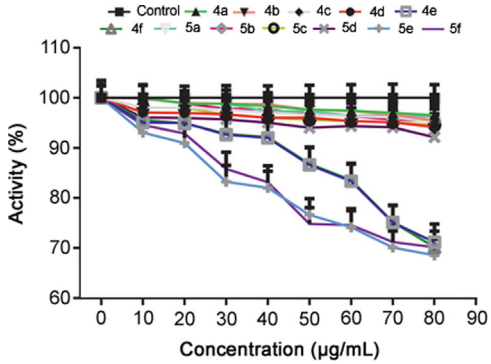

Fig. 3. Concentration-dependent decrease in the percentage activity of STAT3 after treatment with compounds (**4a–5f**) in the Alpha screen based assay.

3.2.4. *Compound 5e inhibited STAT3 activation in Alpha Screen-based assay*

The molecular docking results showed that compound **5e** effectively bound with the SH2 domain of STAT3 protein. Based on that, we further investigated the direct interaction of the compounds (**4a–5f**) with STAT3, for which the compounds were subjected to the Alpha Screen based assay [35] (an in vitro competitive binding assay used to recognize the ability of compounds to directly inhibit the binding of SH2 containing proteins to their respective phosphopeptides). Among all, compound **5e** considerably interacted with the SH2 domain and exhibited significant activity against STAT3 (74.12% of inhibition at 60 µg/mL concentration) (Fig. 3).

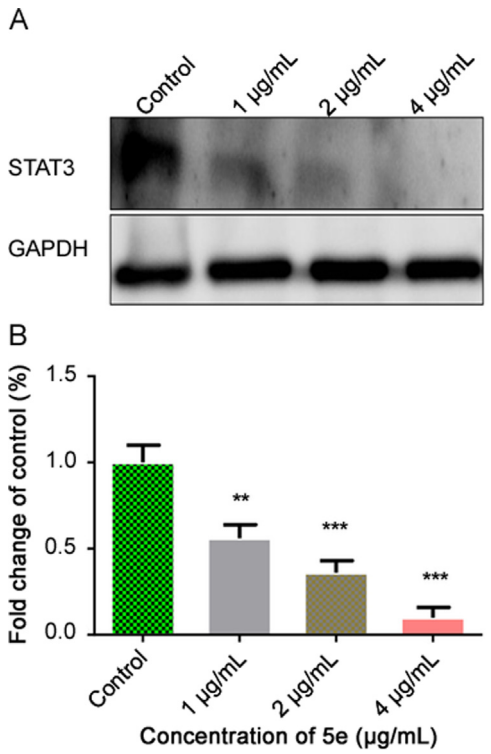

Fig. 4. (A) Western blotting analysis of STAT3 expression in the total protein extract from MCF-7 cells exposed to different concentrations of **5e** for 24 h. (B) Fold changes in the protein expression compared to the loading control GAPDH. Values are expressed as mean ± SD for a set of three experiments. $^{**}P < 0.01$, $^{***}P < 0.001$, compared to control.

3.3. *Compound 5e inhibited expression of STAT3 via Western blot assay*

From previous cytotoxic studies, the IC_{50} value for compound **5e** was found to be 2.45 ± 1.03 µg/mL for MCF-7 cancer cells [1]. Thus, we investigated the effect of compound **5e** on STAT3 in MCF-7 cancer cells at the same concentrations via Western blot assay. The results showed that compound **5e** considerably decreased the expression of STAT3 in a concentration-dependent manner, thus inhibiting its activation (Fig. 4A). The decrease in the folds of protein expression was measured using Image J software (Fig. 4B) [45]. The data collectively suggested that compound **5e** could inhibit STAT3 activation.

4. Conclusion

In this study, we showed that 2, 5-disubstituted-1, 3, 4-oxadiazole derivatives, particularly compound **5e** (5-(aminophenyl)-2-(butylthio)-1,3,4oxadiazole), displayed significant antioxidant activities by potentially scavenging the formed radicals. Additionally, computational studies suggested that the compound **5e** emerged as a lead for inhibition of STAT3, thus providing a new therapeutic approach to cancer drug development. Further optimization of the derivatives needs to be explored.

Acknowledgments

This article has been supported by UGC (University Grant Commission) (F no.- 43-172/2014 (SR)).

Conflicts of interest

The authors declare that there are no conflicts of interest.

References

[1] R. Khanam, K. Ahmad, I.I. Hejazi, et al., Inhibitory growth evaluation and apoptosis induction in MCF-7 cancer cells by new 5-aryl-2-butylthio-1, 3, 4-oxadiazole derivatives, Cancer Chemother. Pharmacol. 80 (2017) 1027–1042.
[2] N. Mihailović, V. Marković, I.Z. Matić, et al., Synthesis and antioxidant activity of 1,3,4-oxadiazole and their diacylhydrazine precursors derived from phenolic acids, RSC Adv. 7 (2017) 8550–8560.
[3] I.I. Hejazi, R. Khanam, S.H. Mehdi, et al., New insights into the antioxidant and apoptotic potential of Glycyrrhiza glabra L. during hydrogen peroxide mediated oxidative stress: an in vitro and in silico evaluation, Biomed. Pharmacother. 94 (2017) 265–279.
[4] A.M. Pisoschi, A. Pop, The role of antioxidants in the chemistry of oxidative stress: a review, Eur. J. Med. Chem. 97 (2015) 55–74.
[5] C. Siquet, F. Paiva-Martins, J.L. Lima, et al., Antioxidant profile of dihydroxy- and trihydroxyphenolic acids – a structure–activity relationship study, Free Radic. Res. 40 (2006) 433–442.
[6] B. Velika, I. Kron, Antioxidant properties of benzoic acid derivatives against superoxide radical, Free Rad. Antioxid. 2 (2012) 62–67.
[7] A. Lukin, R. Karapetian, Y. Ivanenkov, et al., Privileged 1, 2, 4-oxadiazoles in anticancer drug design: novel 5-Aryloxymethyl-1, 2, 4-oxadiazole leads for prostate cancer therapy, Lett. Drug Des. Discov. 13 (2016) 198–204.
[8] M. Swapna, C. Premakumari, S.N. Reddy, et al., Synthesis and antioxidant activity of a variety of sulfonamidomethane linked 1,3,4-oxadiazole and thiadiazoles, Chem. Pharm. Bull. 61 (2013) 611–617.

[9] V.B. Iyer, B. Gurupadayya, B. Inturi, et al., Synthesis of 1,3,4-oxadiazole as promising anticoagulant agents, RSC Adv. 6 (2016) 24797–24807.
[10] Y. Kotaiah, N. Harikrishna, K. Nagaraju, et al., Synthesis and antioxidant activity of 1, 3, 4-oxadiazole tagged thieno [2, 3-d] pyrimidine derivatives, Eur. J. Med. Chem. 58 (2012) 340–345.
[11] S. Viveka, S. Chandra, G.K. Nagaraja, Synthesis, characterization, and pharmacological screening of new 1, 3, 4-oxadiazole derivatives possessing 3-fluoro-4-methoxyphenyl moiety, Mon. Chem. 146 (2015) 207–214.
[12] W. Zhang, T. Ma, S. Li, et al., Antagonizing STAT3 activation with benzo [b] thiophene 1, 1-dioxide based small molecules, Eur. J. Med. Chem. 125 (2017) 538–550.
[13] S. Haftchenary, M. Avadisian, P.T. Gunning, Inhibiting aberrant Stat3 function with molecular therapeutics: a progress report, Anti-Cancer Drugs 22 (2011) 115–127.
[14] Z. Escobar, A. Bjartell, G. Canesin, et al., Preclinical characterization of 3β-(N-acetyl L-cysteine methyl ester)-2aβ, 3-dihydrogaliellalactone (GPA512), a prodrug of a direct STAT3 inhibitor for the treatment of prostate cancer, J. Med. Chem. 59 (2016) 4551–4562.
[15] M.-J. Lai, H.-Y. Lee, H.-Y. Chuang, et al., N-Sulfonyl-aminobiaryls as antitubulin agents and inhibitors of signal transducers and activators of transcription 3 (STAT3) signaling, J. Med. Chem. 58 (2015) 6549–6558.
[16] S. Fletcher, J.A. Drewry, V.M. Shahani, et al., Molecular disruption of oncogenic signal transducer and activator of transcription 3 (STAT3) protein, Biochem. Cell Biol. 87 (2009) 825–833.
[17] S. Fletcher, B.D. Page, X. Zhang, et al., Antagonism of the Stat3–Stat3 protein dimer with salicylic acid based small molecules, ChemMedChem 6 (2011) 1459–1470.
[18] J.E. Darnell, Validating Stat3 in cancer therapy, Nat. Med. 11 (2005) 595–596.
[19] K. Siddiquee, S. Zhang, W.C. Guida, et al., Selective chemical probe inhibitor of Stat3, identified through structure-based virtual screening, induces antitumor activity, PNAS 104 (2007) 7391–7396.
[20] L.M. Christadore, Discovery of a Small Molecule Dihydroquinolinone Inhibitor with Potent Antiproliferative and Aantitumor Activity Results in Catastrophic Cell Division, Boston University, ProQuest Dissertations Publishing,United States, 2013.
[21] N. Jing, Q. Zhu, P. Yuan, et al., Targeting signal transducer and activator of transcription 3 with G-quartet oligonucleotides: a potential novel therapy for head and neck cancer, Mol. Cancer Ther. 5 (2006) 279–286.
[22] S. Dell'Orto, D. Masciocchi, S. Villa, et al., Modeling, synthesis and NMR characterization of novel chimera compounds targeting STAT3, MedChemComm 5 (2014) 1651–1657.
[23] D.-S. Shin, D. Masciocchi, A. Gelain, et al., Synthesis, modeling, and crystallographic study of 3, 4-disubstituted-1, 2, 5-oxadiazoles and evaluation of their ability to decrease STAT3 activity, MedChemComm 1 (2010) 156–164.
[24] K. Matsuno, Y. Masuda, Y. Uehara, et al., Identification of a new series of STAT3 inhibitors by virtual screening, ACS Med. Chem. Lett. 1 (2010) 371–375.
[25] L.C. Green, D.A. Wagner, J. Glogowski, et al., Analysis of nitrate, nitrite, and [15N] nitrate in biological fluids, Anal. Biochem. 126 (1982) 131–138.
[26] L. Marcocci, J.J. Maguire, M.T. Droylefaix, et al., The nitric oxide-scavenging properties of Ginkgo biloba extract EGb 761, Biochem. Biophys. Res. Commun. 201 (1994) 748–755.
[27] R.J. Ruch, S.-j. Cheng, J.E. Klaunig, Prevention of cytotoxicity and inhibition of intercellular communication by antioxidant catechins isolated from Chinese green tea, Carcinogenesis 10 (1989) 1003–1008.
[28] T. Jing, Z. Zhao, The improved pyrogallol method by using terminating agent for superoxide dismutate measurement, Prog. Biochem. Biophys. 1 (1995).
[29] M. Oyaizu, Studies on products of browning reactions: antioxidative activities of products of browning reaction prepared from glucosamine, Jpn. J. Nutr. 44 (1986) 307–315.
[30] P. Prieto, M. Pineda, M. Aguilar, Spectrophotometric quantitation of antioxidant capacity through the formation of a phosphomolybdenum complex: specific application to the determination of vitamin E, Anal. Biochem. 269 (1999) 337–341.
[31] M.F. Ansari, S.M. Siddiqui, K. Ahmad, et al., Synthesis, antiamoebic and molecular docking studies of furan-thiazolidinone hybrids, Eur. J. Med. Chem. 124 (2016) 393–406.
[32] G.M. Morris, Automated docking using a Lamarckian genetic algorithm and an empirical binding free energy function, J. Comp. Chem. 19 (1998) 1639–1662.
[33] K. Ahmad, A. Roouf Bhat, F. Athar, Pharmacokinetic evaluation of callistemon viminalis derived natural compounds as targeted inhibitors against δ-opioid receptor and farnesyl transferase, Lett. Drug Des. Discov. 14 (2017) 488–499.
[34] H.E. Selick, A.P. Beresford, M.H. Tarbit, The emerging importance of predictive ADME simulation in drug discovery, Drug Discov. Today 7 (2002) 109–116.
[35] D. Masciocchi, S. Villa, F. Meneghetti, et al., Biological and computational evaluation of an oxadiazole derivative (MD77) as a new lead for direct STAT3 inhibitors, MedChemComm 3 (2012) 592–599.
[36] P. Singh, F. Bast, High-throughput virtual screening, identification and in vitro biological evaluation of novel inhibitors of signal transducer and activator of transcription 3, Med. Chem. Res. 24 (2015) 2674–2708.
[37] M.A. Sindhe, Y.D. Bodke, R. Kenchappa, et al., Synthesis of a series of novel 2, 5-disubstituted-1, 3, 4-oxadiazole derivatives as potential antioxidant and antibacterial agents, J. Chem. Biol. 9 (2016) 79–90.
[38] G.M. Reddy, A. Muralikrishna, V. Padmavathi, et al., Synthesis and antioxidant activity of styrylsulfonylmethyl 1,3,4-oxadiazole, pyrazolyl/isoxazolyl-1,3,4-oxadiazole, Chem. Pharm. Bull. 61 (2013) 1291–1297.
[39] A.M. Najafabad, R. Jamei, Free radical scavenging capacity and antioxidant activity of methanolic and ethanolic extracts of plum (Prunus domestica L.) in both fresh and dried samples, Avicenna J Phytomed. 4 (2014) 343–353.
[40] S. Sharma, R. Gupta, S.C. Thakur, Attenuation of collagen induced arthritis by centella asiatica methanol fraction via modulation of cytokines and oxidative stress, Biomed Environ Sci. 27 (2014) 926–938.
[41] G. Agelis, A. Resvani, C. Koukoulitsa, et al., Rational design, efficient syntheses and biological evaluation of N, N′-symmetrically bis-substituted butylimidazole analogs as a new class of potent Angiotensin II receptor blockers, Eur. J. Med. Chem. 62 (2013) 352–370.
[42] E. Bendary, R. Francis, H. Ali, et al., Antioxidant and structure–activity relationships (SARs) of some phenolic and anilines compounds, AoAS 58 (2013) 173–181.
[43] S. Becker, B. Groner, C.W. Müller, Three-dimensional structure of the Stat3β homodimer bound to DNA, Nature 394 (1998) 145–151.
[44] X. Liao, X. Zhou, N.K. Mak, et al., Tryptanthrin inhibits angiogenesis by targeting the VEGFR2-mediated ERK1/2 signalling pathway, PLoS One 8 (2013) 82294.
[45] R. Khanam, R. Kumar, I.I. Hejazi, et al., Piperazine clubbed with 2-azetidinone derivatives suppresses proliferation, migration and induces apoptosis in human cervical cancer HeLa cells through oxidative stress mediated intrinsic mitochondrial pathway, Apoptosis 23 (2018) 113–131.